Available online at www.sciencedirect.com
ScienceDirect
Electrochimica Acta 53 (2008) 7514–7522
ELECTROCHIMICA Acta
www.elsevier.com/locate/electacta

EIS analysis on low temperature fabrication of TiO_2 porous films for dye-sensitized solar cells☆

Chao-Po Hsu[a], Kun-Mu Lee[a], Joseph Tai-Wei Huang[b], Chia-Yu Lin[b], Chia-Hua Lee[c], Lih-Ping Wang[c], Song-Yeu Tsai[c], Kuo-Chuan Ho[a,b,*]

[a] *Institute of Polymer Science and Engineering, National Taiwan University, Taipei 10617, Taiwan*
[b] *Department of Chemical Engineering, National Taiwan University, Taipei 10617, Taiwan*
[c] *Photovoltaics Technology Center, Industrial Technology Research Institute, Chutung, Hsinchu 31040, Taiwan*

Received 18 July 2007; received in revised form 29 January 2008; accepted 31 January 2008
Available online 16 February 2008

Abstract

A low temperature (<150 °C) fabrication method for preparation of TiO_2 porous films with high efficiency in dye-sensitized solar cells (DSSCs) has been developed. The Ti(IV) tetraisopropoxide (TTIP) was added to the paste of TiO_2 nanoparticles to interconnect the TiO_2 particles. The electrochemical impedance spectroscopy (EIS) technique was employed to quantify the charge transport resistance at the TiO_2/dye/electrolyte interface (R_{ct2}) and electron lifetime in the TiO_2 film (τ_e) under different molar ratios of TTIP/TiO_2 and also at various TiO_2 thicknesses. It was found that the R_{ct2} decreased as the molar ratio increased from 0.02 to 0.08, however, it increased at a molar ratio of 0.2 due to the reduction in surface area for dye adsorption. In addition, the characteristic frequency peak shifted to lower frequency at a molar ratio of 0.08, indicating the longer electron lifetime. As for the thickness effect, TiO_2 film with a thickness around 17 μm achieved the best cell efficiency. EIS study also confirmed that, under illumination, the smallest R_{ct2} was associated with a TiO_2 thickness of 17 μm, with the R_{ct2} increased as the thickness of TiO_2 film increased. In the Bode plots, the characteristic frequency peaks shifted to higher frequency when the thickness of TiO_2 increased from 17.2 to 48.2 μm, indicating the electron recombination increases as the thickness of the TiO_2 electrode increases.

Finally, to make better use of longer wavelength light, 30 wt% of larger TiO_2 particle (300 nm) was mixed with P25 TiO_2 as light scattering particles. It effectively increased the short-circuit current density and cell conversion efficiency from 7.44 to 8.80 mA cm^{-2} and 3.75 to 4.20%, respectively.

Keywords: Dye-sensitized solar cells; EIS; Low temperature fabrication; TiO_2 film; TTIP

1. Introduction

The dye-sensitized solar cells (DSSCs) have attracted much attention as the next-generation solar cell. It is generally accepted that the low production costs and good efficiency for energy conversion, reaching single cell efficiency of 11% and module efficiency of 7% in some cases [1], will make this technology competitive. The working principle of the DSSC is based upon the injection of electrons from a photoexcited state of the sensitizer into the conduction band of the semiconductor. A charge mediator, i.e., a suitable redox couple, must be added to the electrolyte for reducing the oxidized dye. The mediator also needs to be renewed in the counter-electrode, making the photoelectrochemical cell regenerative.

At the present time, research pursues the development of the inexpensive solar cell based on flexible plastic substrate as the nanocrystalline TiO_2 electrode and counter electrode [2]. However, the conventional method for the preparation of TiO_2 electrodes for DSSCs using colloidal suspensions of TiO_2 nanoparticles includes high-temperature sintering at 450–500 °C, which is necessary to establish a good interconnection between the TiO_2 particles and to remove organic additives

☆ This manuscript has been presented at the Seventh International Symposium on Electrochemical Impedance Spectroscopy, Argelès-sur-Mer, France, June 3–8, 2007.

* Corresponding author at: Department of Chemical Engineering, National Taiwan University, Taipei 10617, Taiwan.
E-mail address: kcho@ntu.edu.tw (K.-C. Ho).

0013-4686/$ – see front matter © 2008 Elsevier Ltd. All rights reserved.
doi:10.1016/j.electacta.2008.01.104

such as precursor or polymer for cementing the connection between TiO_2 particles and the substrate, cannot be applied to prepare films on plastic substrates because plastic substrates structure would crack at such high temperature.

The development of low-temperature fabrication methods should overcome two main problems such as incomplete necking of the particles and presence of residual organics in the film [3]. These problems lower the diffusion coefficient and decrease the lifetime of the electrons. The film revealed a larger inherent resistance than the conventional ones. Recently, some efforts have been made to develop methods compatible with plastic substrate such as electrophoretical deposition [4], gas phase hydrothermal preparation [5], chemical sintering [6], mechanical compression of crystalline particles [7], and sol–gel method with UV/ozone treatment [8].

In this study, we prepared porous TiO_2 film based on sintering of colloids and precursor at a low temperature (150 °C). TTIP mixed with nanocrystalline TiO_2 powder is hydrolyzed and crystallizes into TiO_2 when they are treated by low temperature sintering in the oven. The newly formed TiO_2 acts as "glue" interconnects of the TiO_2 particles as well as that between the film and the substrate [5]. It would improve the connection between TiO_2 particles resulted from the low sintering temperature which caused a poor electric contact between particles in the film.

In addition, electrochemical impedance spectroscopy (EIS) is a useful method for analysis of charge transport process. EIS is a steady state method measuring the current response to the application of an ac voltage as function of the frequency [9]. EIS has been widely employed to study the kinetics of electrochemical and photoelectrochemical processes including the elucidation of salient electronic and ionic processes occurring in the DSSCs [10–13]. In this study, we utilize the EIS not only analyze the charge transport resistance in DSSCs but also fit the curves in Nyquist plots. After obtaining the exact resistance, capacitance and time constant in DSSCs, the effects of low-temperature fabrication parameter of TiO_2 electrodes on DSSCs were discussed.

2. Experimental

2.1. Materials

Anhydrous I_2, ethanol (99.5%), tertiary butanol and 4-tertiary butyl pyridine (TBP) were obtained from Merck and titanium(IV) tetraisopropoxide (TTIP) (+98%) was purchased from Acros and all were used as such. The N3 dye was the commercial product obtained from Solaronix S.A., Aubonne, Switzerland.

2.2. Preparation of TiO_2 electrodes

The preparation of TiO_2 precursor and the electrode fabrication were carried out according to the procedures mentioned in literatures [8]. Degussa P25-TiO_2, titanium(IV) tetraisopropoxide (TTIP), and ethanol were mixed at different molar ratios and dispersed using an ultrasonic horn for 30 min, After stirring for 1 h, the paste was coated on fluorine doped SnO_2-coated conductive glass (FTO glass) by a glass rod. The ethanol evaporated in the air at room temperature after a few minutes. Then the films were sintered at 150 °C for different times.

2.3. The cell assembling of DSSCs

An active area of 0.25 cm^2 was selected from sintered electrode and the electrodes were immersed in 3×10^{-4} M solution of *cis*-di(thiocyanato)bis(2,2′-bipyridyl-4,4′-dicarboxylate)ruthenium (II) (N3 dye) containing acetonitrile and tertiary butanol (in the volume ratio of 1:1) overnight. Pt (100 nm thick) sputtered on FTO was used here as the counter electrode.

The cell was fabricated by applying an ionomer resin (Surlyn 1702, Dupont, a thickness of 50 μm) between the two electrodes. The resin also acts as a spacer and the cell gap was therefore fixed at 50 μm. Two holes were made on the resin and the whole set-up was heated at 100 °C on a hot plate till all the resin had been melted. The electrolyte was then injected into the space between the electrodes through these two holes. Finally, these two holes were sealed completely by the Torr Seal® cement (Varian, MA, USA). The electrolyte was composed of 0.8 M 1-methyl-3-propylimidazolium iodide (MPII)/0.1 M LiI/0.05 M I_2/0.5 M TBP in CH_3CN.

2.4. Instruments and measurements

The photoelectrochemical characterizations of the DSSCs were carried out by using an AM 1.5 simulated light radiation (1 sun). The light source was a 450 W Xe lamp (Oriel, #6266) equipped with a water-based IR filter and AM 1.5 filter (Oriel, #81075). UV–vis absorption data were measured by an UV–vis spectrophotometer (Jasco, V-570). Photoelectrochemical characteristics and the electrochemical impedance spectroscopy (EIS) measurements of the DSSCs were recorded with a potentiostat/galvanostat (PGSTAT 30, Autolab, Eco-Chemie, the Netherlands) under 100 mW cm^{-2}. The frequency range was explored from 10 mHz to 65 kHz. The applied bias voltage and ac amplitude were set at open-circuit voltage of the DSSCs and 10 mV between the FTO-Pt counter electrode and the FTO-TiO_2-dye working electrode, respectively, starting from the short-circuit condition [14]. The impedance spectra were analyzed by an equivalent circuit model interpreting the characteristics of the DSSCs [15]. The photovoltage transients of assembled devices were recorded with a digital oscilloscope (LeCroy, model LT322). Pulsed laser excitation was applied by a frequency-doubled Q-switched Nd:YAG laser (Spectra-Physics laser, model Quanta-Ray GCR-3-10) with 2 Hz repetition rate at 532 nm, and 7 ns pulse width at half-height. The beam size was slightly larger than 0.25 cm^2 to cover the area of the device with an incident energy of 1 mJ/cm^2. The average electron lifetime (τ_e) can be estimated from a near-linear fitting of the photovoltage in a logarithmic scale against the lapsed time.

3. Results and discussion

3.1. The effects of different TTIP/TiO_2 molar ratios on the performance of DSSCs

To optimize the molar ratio of TTIP with respect to TiO_2 powder for film preparation, the films made up of pastes with different TTIP concentrations were investigated. In this study, TTIP not only was used as the precursor which effectively binds the TiO_2 nanoparticles together, but also used to control the viscosity of the TiO_2 paste. We had prepared the TiO_2 paste under the same experimental condition, except without adding TTIP, however, the TiO_2 film such prepared had very weak adhesion properties and peeled off easily from the conducting glass. Therefore, we do not present the data for the zero ratio of TTIP/TiO_2 in this study. The properties of TiO_2 films with different molar ratios of TTIP/TiO_2 between 0.02 and 0.20 were measured. The change of their surface parameters and cell performances are given in Table 1. When the TTIP/TiO_2 molar ratio was increased from 0.02 to 0.20, it was found that the interconnections were poor among TiO_2 particles at molar ratio of 0.02 and the best result was obtained at the molar ratio of 0.08, as judged by the cell efficiency. At this condition, the surface area and the pore diameter were measured as 46.7 $m^2\ g^{-1}$ and 11.0 nm, respectively. Higher molar ratios not only led to the formation of amorphous TiO_2 in large quantity around the P25 TiO_2 particles but also decreased the pore diameter from 11.0 to 6.9 nm. Consequently, it became difficult for I^-/I_3^- ions to diffuse into the inner pore of TiO_2 electrode to reduce the oxidized dyes, resulting in poor conversion efficiency. This observation could be explained by the fact that the pores with a diameter of about 7 nm, in which 3 nm is occupied by the N3 dye molecules and leaves an aperture of only 3–4 nm for the diffusion of the electrolyte. This size is only slightly larger than the size of the I_3^- ion, however, if one considers the solvation shell of the ions and Fick's law of diffusion maybe not valid [16].

From the BET data, when the molar ratios increased from 0.02 to 0.08, surface areas did not vary significantly, which were around 47–49 $m^2\ g^{-1}$, and the pore diameters have slightly decreased from 11.8 to 11.0 nm. However, when the TTIP/TiO_2 ratio was increased to 0.20, the TiO_2 particles turned to flake and thus reducing the surface area to 36.8 $m^2\ g^{-1}$ as well as the pore diameter 6.9 nm. The morphology of TiO_2 film prepared at optimized molar ratio of 0.08 was studied with the aid of SEM images and the corresponding pictures are shown in Fig. 1. The results depict similarity to that film prepared by the conventional method such as prepared by annealing under 500 °C. Its high porosity and high surface area caused the increase in amount of adsorbed dyes and the photocurrent. However, the film obtained at molar ratio of 0.20 had larger amount of amorphous TiO_2 due to the ambient hydrolysis of TTIP, which ultimately decreased the surface area and pore diameter of the film. Hence, the addition of optimum TTIP in TiO_2 powder is to cover the surface of TiO_2 particles and to promote the good interconnection. It

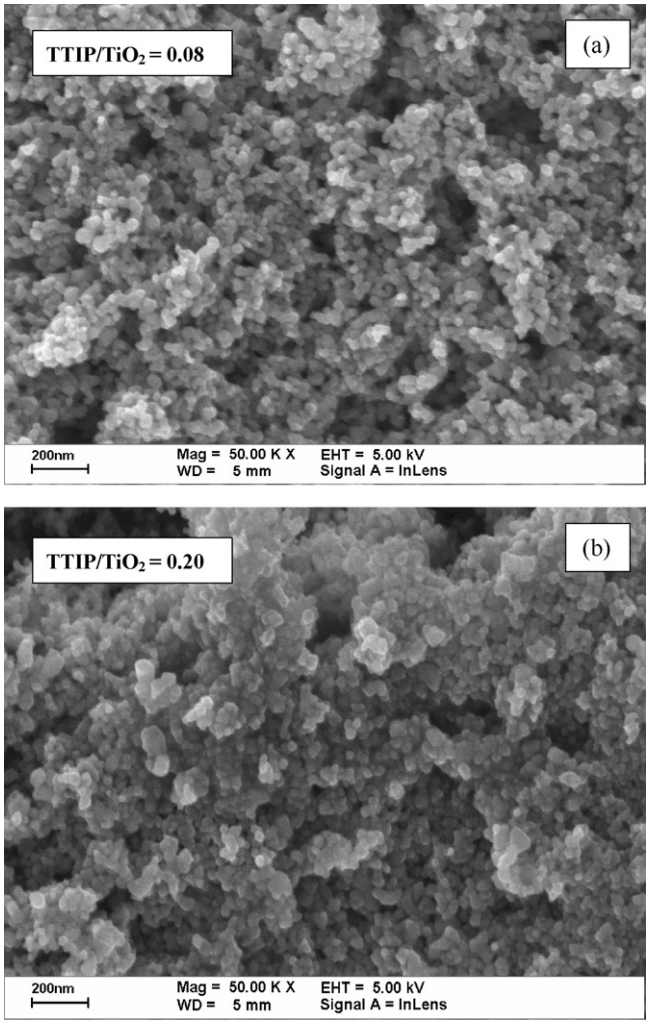

Fig. 1. SEM images of TiO_2 electrodes prepared in different TTIP/TiO_2 molar ratios (a) 0.08 and (b) 0.20.

Table 1
The BET data, electron lifetimes and cell performances of DSSCs (measured under 100 mW cm^{-2}) based on different TTIP/TiO_2 molar ratios in the paste used for TiO_2 electrode preparation

TTIP/TiO_2 (molar ratio)	Surface area[a] ($m^2\ g^{-1}$)	Pore diameter[a] (nm)	τ_e[b] (ms)	J_{SC}[c] (mA cm^{-2})	V_{OC}[c] (V)	FF[c]	η[c] (%)
0.02	48.4	11.8	1.43	3.58	0.746	0.67	1.80
0.04	47.8	11.2	1.86	5.73	0.782	0.72	3.22
0.08	46.7	11.0	1.97	6.08	0.770	0.70	3.28
0.20	36.8	6.9	0.94	1.33	0.622	0.63	0.52

[a] Measured by BET.
[b] The average electron lifetime (τ_e) in the TiO_2 electrode was obtained from the laser induced photovoltage transient technique.
[c] The thickness of TiO_2 film was about 9 μm.

was expected that the TTIP was completely converted into TiO_2 after annealing to transport electrons rapidly which obtained from excited dyes so as to have longer electron lifetime.

Furthermore, using electrochemical impedance spectroscopy (EIS) the internal resistances and the electron transport kinetics of the TiO_2 films in DSSCs were also studied. Fig. 2(a) and (b) shows the Nyquist plots of the electrochemical impedance spectra of the DSSCs for different TTIP/TiO_2 ratios measured under 100 mW cm^{-2}, and the equivalent circuit is shown as the inset of Fig. 2(a). Generally, all the spectra of DSSCs exhibit three semicircles, which are assigned to electrochemical reaction at the Pt counter electrode, charge transfer at the TiO_2/dye/electrolyte and Warburg diffusion process of I^-/I_3^- [14,15]. In our case, it was found that the charge transport resistance at the TiO_2/dye/electrolyte interface (R_{ct2}) decreased as the molar ratio of TTIP/TiO_2 was varied from 0.02 to 0.08 (as seen in Fig. 2(b), which is enlarged from Fig. 2(a)), and increased at a molar ratio of 0.20. This phenomenon may be due to decrease in pore size of TiO_2 film and thus decreasing the dye adsorption as well as penetration of redox couples into the pores of TiO_2 electrode (Fig. 2(a)). Correspondingly, the characteristic frequency peaks (1–10^3 Hz) in Bode phase plots were shown in Fig. 2(c). The characteristic frequency peak shifted to lower frequency when the molar ratio increased to 0.08 and then shifted back again to higher frequency when the ratio was 0.20. The characteristic frequency can be related to as the inverse of the recombination lifetime (τ_r), or electron lifetime (τ_e) in TiO_2 film [17–19]. This implies that a molar ratio of 0.08 has the longer electron lifetime in the TiO_2 film. From the results, it is found that the TiO_2 film prepared at the ratio of 0.20 not only has a higher transport resistance but also has a lower electron lifetime in TiO_2 electrode.

It is generally accepted that the average electron lifetime can be estimated by fitting a decay of the open-circuit voltage transient with $\exp(-t/\tau_e)$, where t is the time and τ_e is an average time constant before recombination. For comparison, the effect of molar ratio on the average electron lifetime was studied by the laser induced photovoltage transient technique. The results are shown in Fig. 3 with *Y*-axis plotted in a logarithmic scale. It can be seen that a near-linear fitting has been satisfied, thus the average electron lifetime can be obtained from the slope. It was found that the electron lifetimes (τ_e) in TiO_2 films enhanced from 1.43 to 1.92 ms when the molar ratio increased from 0.02 to 0.08. Further increase of the molar ratio to 0.20, the τ_e decreased sig-

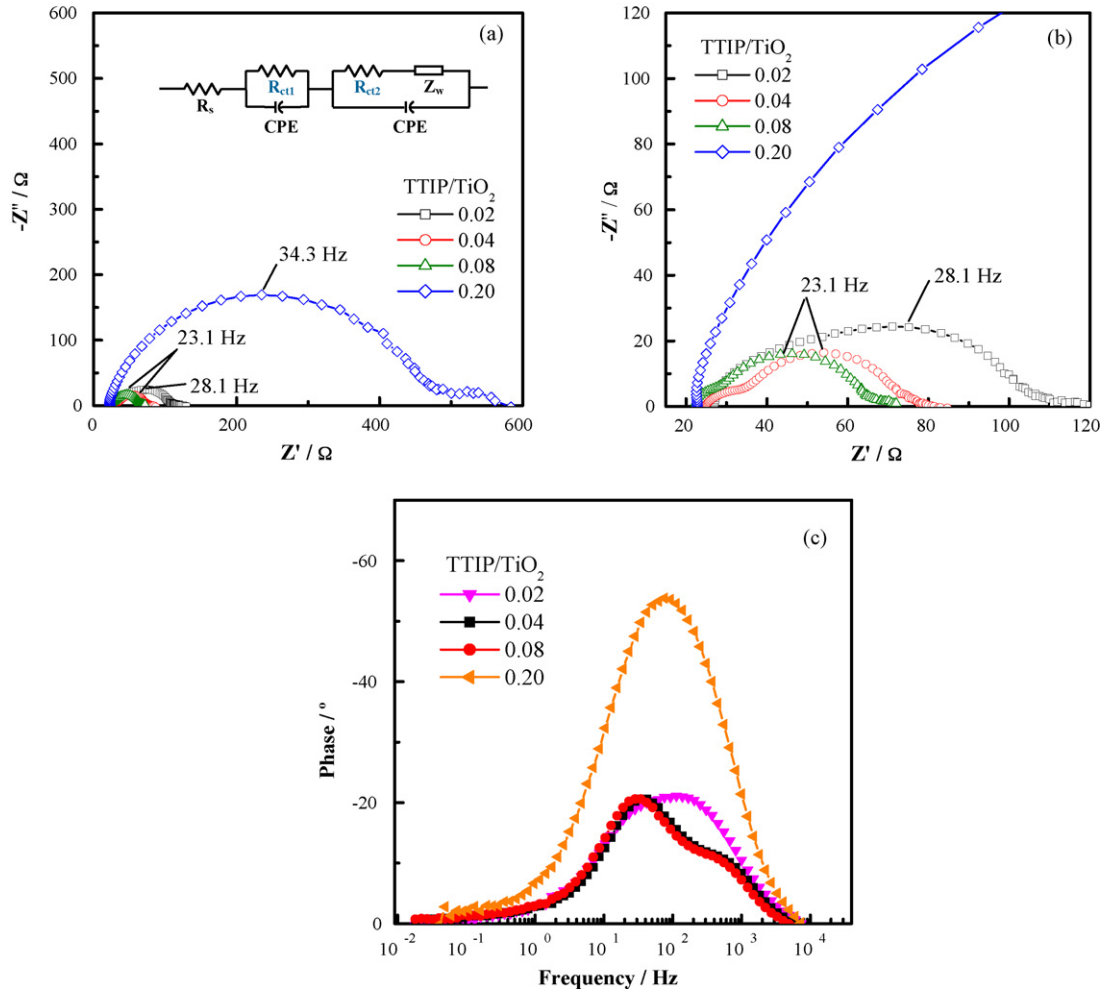

Fig. 2. Electrochemical impedance spectra of DSSCs based on different TTIP/TiO_2 molar ratios measured at V_{OC}, 100 mW cm^{-2}. (a) and (b) are Nyquist plots. (b) Shows an enlargement of (a). (c) Shows Bode phase plot. The equivalent circuit of this study is shown in the inset of (a).

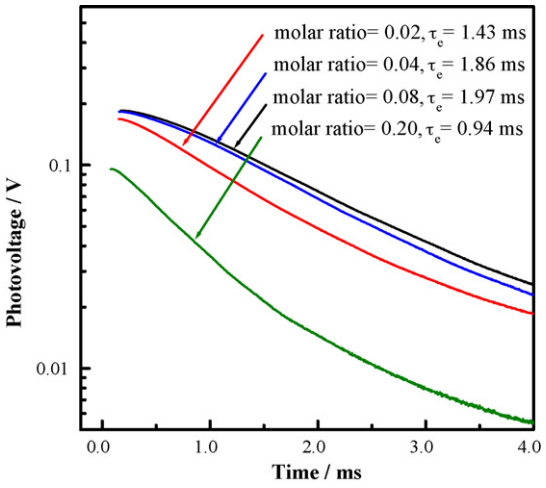

Fig. 3. Transient photovoltage measurements of various TiO_2 electrodes prepared with different molar ratios of TTIP/TiO_2.

nificantly to 0.94 ms. This result is consistent with the previous results obtained from cell performance and EIS analysis.

Electrochemical impedance was also measured in the dark to elucidate the correlation of electron transport with different molar ratios. In these cells, the electrons were transported through the mesoscopic TiO_2 network and react with I_3^-. At the same time, I^- was oxidized to I_3^- at the counter electrode. Hence, the net current was largely dependent on the applied bias. The fitted data of the electron transport resistances and the capacitances obtained from the Nyquist plots at various molar ratios measured under different biases are plotted in Fig. 4(a) and (b), respectively. The time constant can be calculated by Eq. (1):

$$\tau_n = R_{ct2} \times C_\mu \quad (1)$$

where R_{ct2} and C_μ are the charge transport resistance and the chemical capacitance at TiO_2/dye/electrolyte interface, respectively. The chemical capacitance (C_μ) is an equilibrium property that relates the variation of the carrier density to the displacement of the Fermi level. C_μ is a positive quantity, as it represents the equilibrium property.

It can be seen that the ratios of 0.04 and 0.08 reached higher resistances than the others measured in the dark (Fig. 4(a)), indicating the DSSCs based on TTIP/TiO_2 ratios of 0.04 or 0.08 have less recombination and higher open-circuit voltage (V_{OC}). The cell capacitances for all TTIP/TiO_2 ratios increased

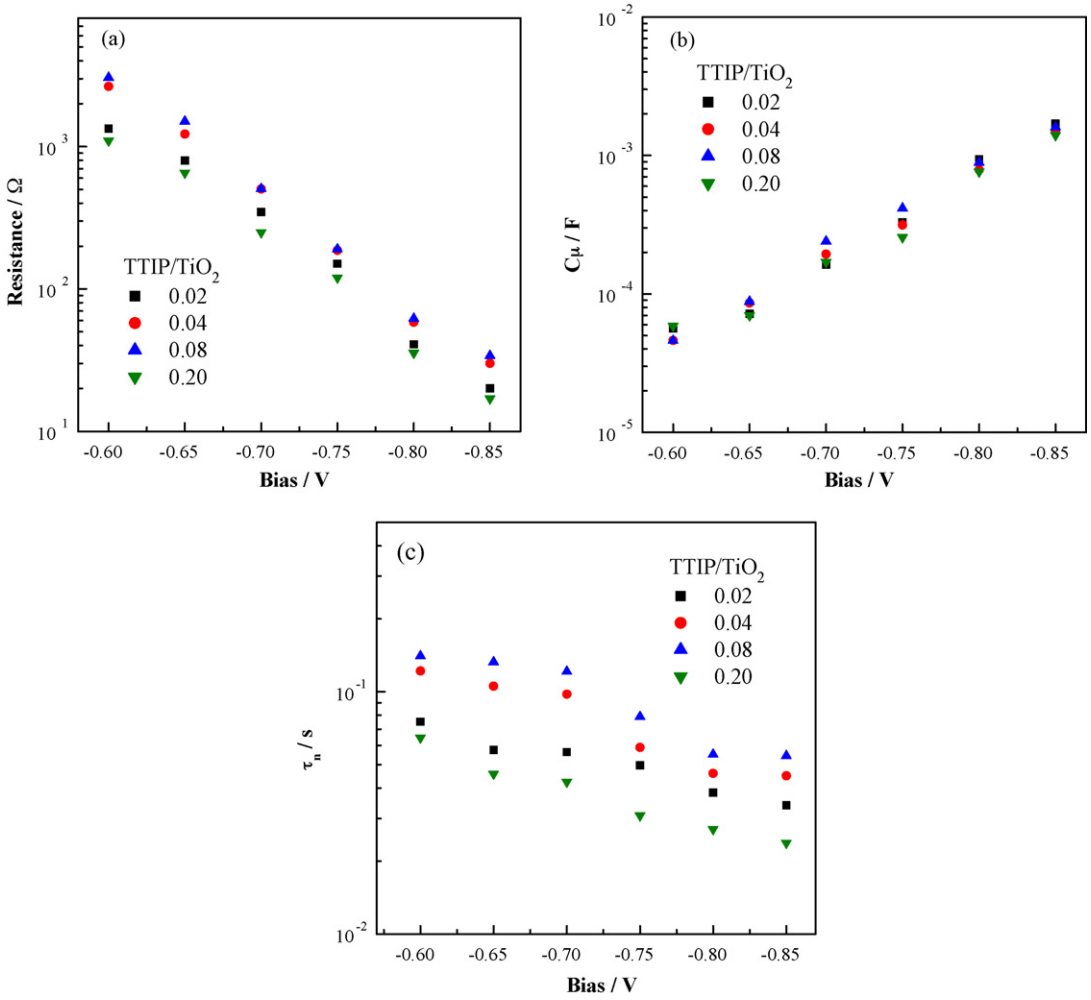

Fig. 4. (a) Electron transport resistance, (b) capacitance, and (c) time constant of DSSCs based on different TTIP/TiO_2 molar ratios were obtained from impedance measurement in the dark by applying various biases.

Table 2
The dye loading, electron lifetimes and cell performances of DSSCs (measured under 100 mW cm^{-2}) based on different thickness of TiO_2 electrodes

Thickness of TiO_2 (μm)	Dye loading (10^{-7} mol cm^{-2})	τ_e[a] (ms)	J_{SC} (mA/cm^{-2})	V_{OC} (V)	FF	η (%)
6.3	0.81	N/A	4.82	0.780	0.73	2.74
17.2	1.20	1.92	7.44	0.760	0.67	3.69
23.7	1.52	1.69	7.01	0.719	0.63	3.17
48.2	2.13	1.46	2.22	0.662	0.76	1.12

[a] The average electron lifetime (τ_e) in the TiO_2 electrode was obtained from the laser induced photovoltage transient technique.

with the increase of the bias (Fig. 4(b)). The time constants increased with the increase of the forward bias. It is interesting to note that higher time constant was observed at the ratio of 0.08 than the other ratios as shown in Fig. 4(c), which confirmed the devices containing TiO_2 electrode with molar ratio of 0.08 had larger time constant due to slower recapture of conduction band electrons by I_3^-. This finding is consistent with our previous argument.

3.2. The effects of TiO_2 electrode thickness on the performance of DSSCs

As for the thickness effect, the variation of dye loading and photovoltaic characteristics such as J_{SC}, V_{OC}, fill factor (FF) and the conversion efficiency (η) are summarized in Table 2. It was noted that the dye loading increased from 0.81×10^{-7} to 2.13×10^{-7} mol cm^{-2} as the thickness of TiO_2 films is increased from 6.3 to 48.2 μm. However, the TiO_2 film with a thickness around 17 μm achieved the best cell efficiency of 3.69%, and further increasing of the thickness caused the lowering of the short circuited current density (J_{SC}), the open-circuit voltage (V_{OC}) and the conversion efficiency (η). That is, although larger film thickness tends to increase the amount of dye adsorption, it also causes higher electron transport resistance and increases the recombination of electron with I_3^- on the TiO_2 surface, resulting in smaller V_{OC} and η. It is noticed that when the thickness of TiO_2 film is larger than 48 μm, the film starts to peel off, resulting in the decrease of the current density to only of 2.22 mA cm^{-2}.

EIS study also confirms the above results under illumination that the smallest R_{ct2} is associated with a TiO_2 thickness of 17.2 μm. With the increase in the thickness of TiO_2 film, the capacitance and R_{ct2}, which were fitted from the Nyquist plot, were increased (Fig. 5(a)). In the Bode phase plot, the characteristic frequency peaks shifted to higher frequency, which means a lower electron lifetime is obtained when the thickness of TiO_2 is increased from 17.2 to 48.2 μm (Fig. 5(b)). This observation implies that with the increase in the thickness of TiO_2 electrode, the electron transport encountered a longer distance and is easier to recombine with I_3^-, thus increasing the electron transfer resistance and decreasing the electron lifetime in the TiO_2 film.

Similarly, the laser induced photovoltage transient technique was also used. The electron lifetimes were found to be 1.92, 1.69 and 1.46 ms for 17.2, 23.7 and 48.2 μm of TiO_2 electrode thickness, respectively. Those data are included in Table 2. This observation is rationalized in terms of an increase in the number of traps encountered by the conduction band electrons with increasing TiO_2 film thickness. This slows down the electron motion, thus lowering the electron collection efficiency [20].

3.3. The effect of light intensity on the performance of DSSCs

We also have investigated the effect of light intensity on the performance of DSSCs by using EIS. Fig. 6 shows the impedance spectra of DSSCs with TiO_2 electrode prepared at

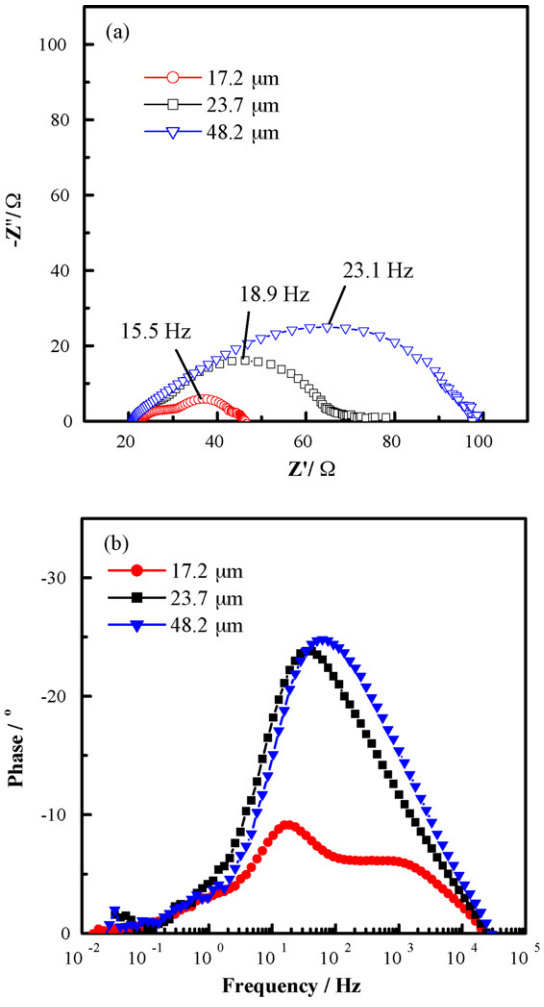

Fig. 5. Electrochemical impedance spectra of DSSCs based on various thickness of TiO_2 electrodes measured at V_{OC}, 100 mW cm^{-2}. (a) Nyquist plot and (b) Bode phase plot.

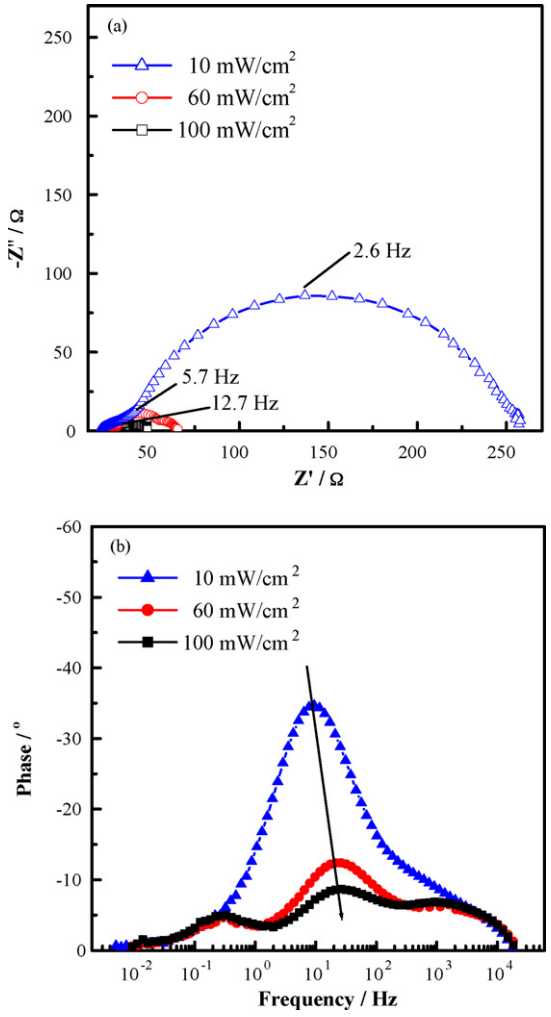

Fig. 6. Electrochemical impedance spectra of DSSC based on TTIP/TiO_2 molar ratio of 0.08 and the TiO_2 thickness of 17.2 μm measured under 10, 60, and 100 mW cm^{-2}. (a) Nyquist plot and (b) Bode phase plot.

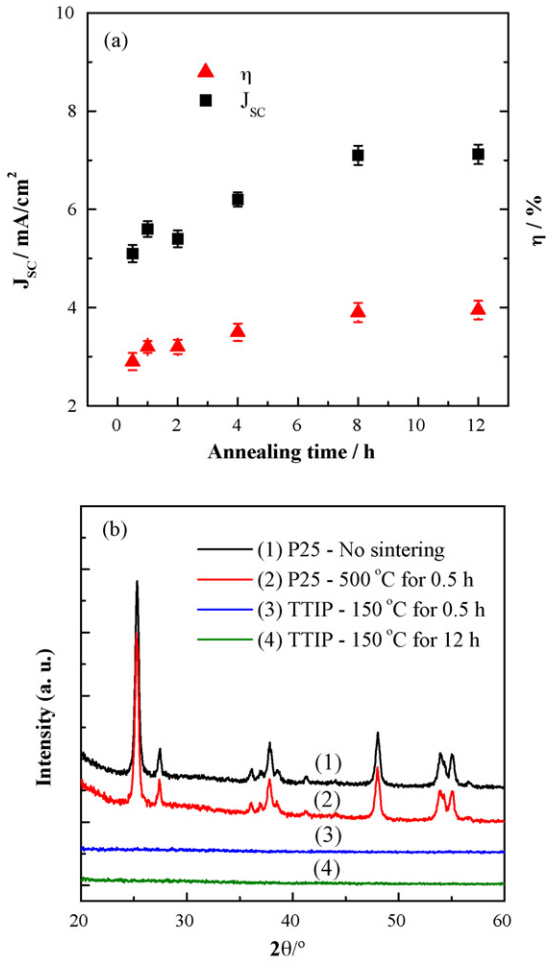

Fig. 7. (a) The variation of current density and cell conversion efficiency of DSSCs based on the TiO_2 electrode treatment at 150 °C for various annealing times up to 12 h. (b) The XRD patterns of P25 TiO_2 without and with sintering at 500 °C for 0.5 h are shown, respectively, in curves (1) and (2). The XRD patterns of TiO_2 film obtained from the TTIP precursor and sintered at 150 °C for 0.5 h and 12 h are shown, respectively, in curves (3) and (4).

a molar ratio of 0.08 and a thickness of 17.2 μm under different light intensities. The results indicated that R_{ct2} decreased (Fig. 6(a)) and the characteristic frequency peaks (Fig. 6(b)) also shifted to higher frequency as the light intensity is increased. Those results suggested that more electrons are injected into the TiO_2 electrode, but the injected electrons are lost more rapidly with the increase in the light intensity. Meanwhile, under illumination, V_{OC} can be expressed as [10,21]:

$$V_{OC} = \frac{RT}{\beta F} \ln\left(\frac{AI}{n_0 k_1 [I_3^-] + n_0 k_2 [D^+]}\right) \quad (2)$$

where k_1 and k_2 being the kinetic constants of back reaction of injected electrons with triiodide and recombination of these electrons with oxidized dye, respectively, and n_0 being the concentration of accessible electronic states in the conduction band. Neglecting the loss term due to recombination with the oxidized dye molecules, V_{OC} depends logarithmically on the inverse concentration of I_3^- and increases with incident photo flux I. The V_{OC} of DSSCs measured at the molar ratio of 0.08 and 17.2 μm of TiO_2 electrode under 100, 60 and 10 mW cm^{-2} illuminations were found to be 0.760, 0.735 and 0.695 V, respectively, following the predicted logarithmical relation. Any variations of the local triiodide concentration due to light illumination appear to have a small effect [10].

3.4. Optimization on the TiO_2 electrode and DSSC performance

It is important to study the effect of annealing time on the performances of DSSCs. Hence, the TiO_2 films annealed at 150 °C under various times were studied. The short-circuited current density and conversion efficiency increased gently with the increase in the annealing time as shown in Fig. 7(a). The crystallinity of the P25 TiO_2 powder with and without annealing at 500 °C and the crystallinity of TiO_2 film obtained from the TTIP precursor, which is to imitate the thin film material covered on P25 TiO_2 particles to increase the interconnection between TiO_2 particles, treated at 150 °C for both 0.5 and 12 h were analyzed by XRD and shown in Fig. 7(b). It was found that there were no

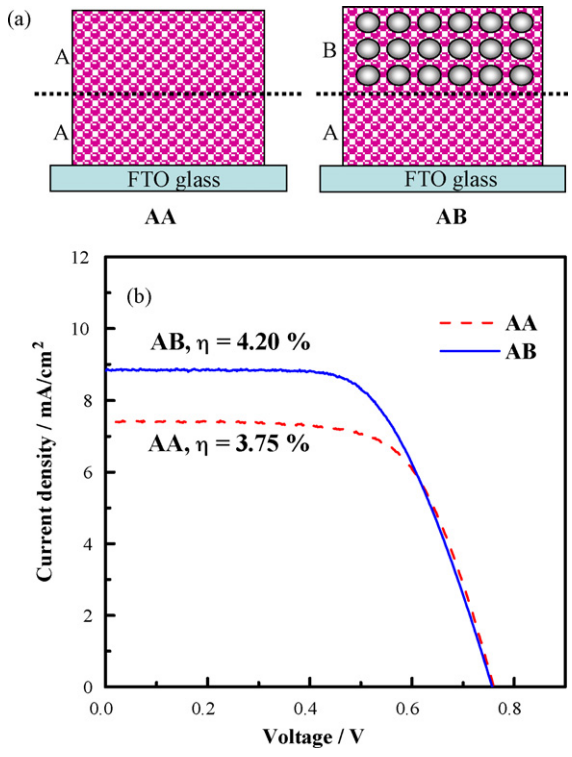

Fig. 8. (a) The sketch plots of different collocations of TiO_2 electrodes. (b) *I–V* curves of DSSCs based on different collocations of TiO_2 electrodes.

changes in XRD patterns for P25 TiO_2 powders before and after annealing at 500 °C. Also, the TiO_2 films obtained from the TTIP precursor are amorphous. These observations suggested that the enhancement of the cell performance is due to neither the heat treatment of P25 TiO_2 particles at 500 °C nor the formation of crystalline TiO_2 film from the TTIP precursor. It is vary likely due to the decomposition of organics originating from the TTIP on the TiO_2 surface after thermal treatment like the treatment of UV/ozone [8].

Finally, in order to develop high efficiency DSSCs, the tuning of TiO_2 photo electrode's morphology towards optimization has to be taken into account. To reduce the light loss ascribed to the back scattering, double layer film with light scattering particle has been shown to achieve better performance [22,23]. In this study, TiO_2 films were fabricated by mixing up of nano-particles (~25 nm) and large particles (300 nm) at a weight ratio of 7:3. Finally, the cell performances were compared for different types of TiO_2 films such as: film contains (i) only nano-particles (case AA in Fig. 8(a)) and (ii) first layer nanoparticle and second layer mixture of both (case AB in Fig. 8(a)). Both configurations are shown in Fig. 8(a). The cell fabricated using this double layer film (AB), which including light scattering particles in TiO_2 electrode as the working electrode could increase the J_{SC} ~19% which from 7.44 to 8.84 mA cm^{-2} due to decrease the loss of light ascribed to the back-scattering, and achieved a high cell conversion efficiency of 4.20%. This result is evidently better than that of the cell fabricated without using light scattering particles (Fig. 8(b)).

4. Conclusions

A low temperature fabrication method for preparation of TiO_2 porous films on conducting glass substrate with high cell efficiency in the DSSC has been developed. TiO_2 film with a molar ratio of 0.08 and a thickness around 17 μm achieved the best cell efficiency. The EIS technique was employed to quantify the charge transport resistance and electron lifetime. The charge transport resistance at the TiO_2/dye/electrolyte interface (R_{ct2}) decreased as a function of the molar ratio of TTIP/TiO_2 from 0.02 to 0.08, and the TiO_2 film prepared with a molar ratio of 0.08 also shows the longest electron lifetime. As for the thickness effect, the smallest R_{ct2} was associated with a TiO_2 thickness of 17 μm, and when the thickness of TiO_2 is increased from 17.2 to 48.2 μm, the characteristic frequency peaks shifted to higher frequency and increased in the electron recombination was also noticed.

Due to the decomposition of organics originating from the TTIP on the TiO_2 surface, the cell conversion efficiency increases gently with the annealing. Finally, adding 30 wt% of larger TiO_2 particle into TiO_2 nanoparticles as light scattering particles could enhance the photocurrent density and cell conversion efficiency of 8.81 mA cm^{-2} and 4.20%, respectively.

Acknowledgements

This work was financially supported by the Academia Sinica, Taipei, Taiwan, under Grants AS-94-TP-A02 and AS-97-TP-A08. This work was also partially supported by the National Research Council of Taiwan, under Grant NSC 96-2120-M-002-016.

References

[1] M. Grätzel, Nature 414 (2001) 338.
[2] S.A. Haque, E. Palomares, H.M. Upadhyaya, L. Otley, R.J. Potter, A.B. Holmes, J.R. Durrant, Chem. Commun. (2003) 3008.
[3] C. Longo, A.F. Nogueira, M.A. De Paoli, H. Cachet, J. Phys. Chem. B 106 (2002) 5925.
[4] T. Miyasaka, Y. Kijitori, T.N. Murakami, M. Kimura, S. Uegusa, Chem. Lett. (2002) 1250.
[5] D. Zhang, T. Yoshida, K. Furuta, H. Minoura, J. Photochem, Photobiol. A: Chem. 164 (2004) 159.
[6] N.G. Park, K.M. Kim, M.G. Kang, K.S. Ryu, S.H. Chang, Y.J. Shin, Adv. Mater. 17 (2005) 2349.
[7] G. Boshloo, H. Lindstrom, E. Magnusson, A. Holmberg, A. Hagfeldt, J. Photochem, Photobiol. A: Chem. 148 (2002) 11.
[8] D. Zhang, T. Yoshida, T. Oekermann, K. Furuta, H. Minoura, Adv. Funct. Mater. 16 (2006) 1228.
[9] M.J. Ross, K.R. William, Impedance Spectroscopy: Emphasizing Solid Materials and Systems, John Wiley & Sons, New York, 1987.
[10] Q. Wang, J.E. Moser, M. Grätzel, J. Phys. Chem. B 109 (2005) 14945.
[11] N. Papageorgiou, W.F. Maier, M. Grätzel, J. Electrochem. Soc. 144 (1997) 876.
[12] J. Bisquert, J. Phys. Chem. B 106 (2002) 325.
[13] A. Hauch, A. Georg, Electrochim. Acta 46 (2001) 3457.
[14] C. Longo, J. Freitas, M.A. De Paoli, J. Photochem, Photobiol. A: Chem. 159 (2003) 33.

[15] M.C. Bernard, H. Cachet, P. Falaras, A. Hugot-Le Goff, M. Kalbac, I. Lukes, N.T. Oanh, T. Stergiopoulos, I. Arabatzis, J. Electrochem. Soc. 150 (2003) E155.
[16] C.J. Barbé, F. Arendse, P. Comte, M. Jirousek, F. Lenzmann, V. Shklover, M. Grätzel, J. Am. Ceram. Soc. 80 (1997) 3157.
[17] G. Schlichthorl, S.Y. Huang, J. Sprague, A.J. Frank, J. Phys. Chem. B 101 (1997) 8141.
[18] G. Schlichthorl, N.G. Park, A.J. Frank, J. Phys. Chem. B 103 (1999) 782.
[19] R. Kern, R. Sastrawan, J. Ferber, R. Stangl, J. Luther, Electrochim. Acta 47 (2002) 4213.
[20] D. Kuang, S. Ito, B. Wenger, C. Klein, J.E. Moser, R. Humphry-Baker, S.M. Zakeeruddin, M. Grätzel, J. Am. Chem. Soc. 128 (2006) 4146.
[21] M. Koelsch, S. Cassaignon, C. Ta Thanh Minh, J.F. Guillemoles, J.P. Jolivet, Thin Solid Films 451–452 (2004) 86.
[22] K.M. Lee, V. Suryanarayanan, K.C. Ho, Solar Energy Mater. Solar Cells 90 (2006) 2398.
[23] Z.S. Wang, H. Kawauchi, T. Kashima, H. Arakawa, Coord. Chem. Rev. 248 (2004) 1381.